information; some instruments provide both. For example, an electron microprobe can be fitted with a secondary electron detector to provide the investigator with excellent high-magnification images of crystal morphology as well as detailed chemical analyses.

TECHNIQUE OVERVIEW

Single-crystal X-ray diffraction techniques are most commonly used in the determination of crystal structures, unit cell sizes, atomic parameters, and bond distributions. Powder X-ray diffraction is a rapid and commonly available technique for mineral identification and can also provide information about unit cell sizes. X-ray fluorescence is a sensitive technique for obtaining chemical analyses of bulk samples including low-abundance elements. High-energy electrons, accelerated from 10 KeV to over 150 KeV, form the basis for numerous electron beam methods. The scanning electron microscope (SEM) provides images of crystal morphology at the micrometer level. Transmission electron microscopes (TEMs) allow for the direct imaging of crystal structures, defects in the structures, and extremely fine-grained intergrowths of different minerals or mineral reactions that are not visible using lower-resolution techniques, such as optical microscopy. Electron diffraction results (as part of TEM techniques) commonly complement structural data obtained from X-ray single crystal experiments. The high-resolution transmission electron microscope (HRTEM) mode allows for the projection of structures on a two-dimensional image with a resolution of about 1.5 Å. Atomic force microscopy (AFM) allows for the characterization of surfaces of minerals on an atomic or near-atomic scale. However, the overviews presented here are inadequate for a thorough understanding of all of the underlying concepts and additional references are given.

Several analytical techniques are specifically designed to obtain *quantitative* chemical data whereas others are best used for *qualitative* data. A **qualitative** analysis involves the detection and identification of all the chemical constituents of a compound ("What is present?"). A **quantitative** analysis involves the determination of the weight percentages (or parts per million composition) of all elements in a compound ("How much of each is present?"). A preliminary *qualitative* analysis is commonly helpful in deciding on the methods to be followed in a subsequent *quantitative* analysis.

Prior to 1947, quantitative chemical analyses of minerals were obtained mainly by "wet" analytical techniques, in which the mineral was dissolved by some appropriate acid. Subsequently, each constituent element was precipitated out of solution and weighed, with results reported as weight percentage of the oxides. Since 1960, the majority of quantitative analyses have been made by instrumental techniques, such as electron microprobe analysis (EMPA) for *in situ* chemical analyses of areas as small as 1 micrometer in diameter (1 μm = 10^{-6}m) and/or X-ray fluorescence analysis (XRF) for chemistry of bulk samples. Secondary ion mass spectrometry (SIMS) uses a focused ion beam to excavate ions from a mineral surface and analyzes their mass and charge with a mass spectrometer. Each of these techniques has its own specific sample preparation requirements and has well-established detection limits, precision, and accuracy values and error ranges. The results of any chemical analysis are generally presented in a table of weight percentages of the elements or oxide components in the mineral analyzed.

TECHNIQUES THAT USE X-RAYS

X-RAY DIFFRACTION TECHNIQUES (XRD)

Since the discovery of X-rays by Wilhelm Conrad Roentgen in 1895, and the first application of an X-ray experiment to the study of crystalline material in 1912 by Max von Laue (see Chapter 1), X-ray diffraction techniques have been fundamental to *crystal structure analysis*. Current knowledge of the location of atoms, their sizes, and their bonding in crystal structures, as well as a structure's space group symmetry and chemical composition and size of its unit cell, has been derived largely from single crystal X-ray diffraction studies. X-ray crystallography is a science that is pursued by researchers with a broad knowledge base in mathematics, physics, chemistry, and computational methods.

This section briefly introduces X-rays and their diffraction effects, followed by a short overview of crystal structure analysis, using *single-crystal techniques* and an introduction to the *X-ray powder diffraction method*, which is routinely used in mineral identification. This quick and inexpensive identification method is especially powerful in the study of minerals (and other materials) that are too fine-grained to be evaluated by optical microscopy. Examples of such materials are members of the clay mineral and zeolite groups. Powder diffraction equipment is generally available in many geology and chemistry departments, as well as industrial laboratories, and is widely used for the study of minerals.

X-ray Spectra

Electromagnetic waves form a continuous series ranging in wavelength from long radio waves with wavelengths of the order of thousands of meters to cosmic

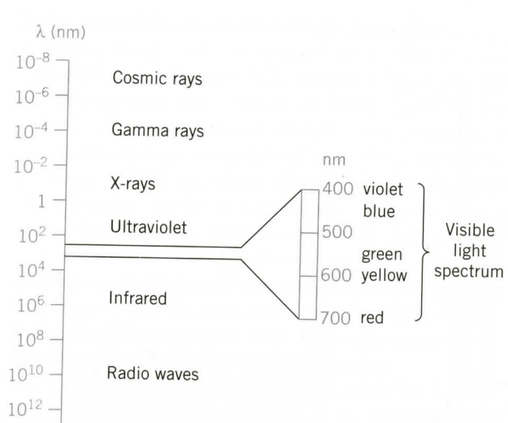

FIG. 14.1 The electromagnetic spectrum with the visible region expanded. Wavelength (λ) values are expressed in nm (nanometers), where 1 nm = 10 Å = 10^{-9} meters.

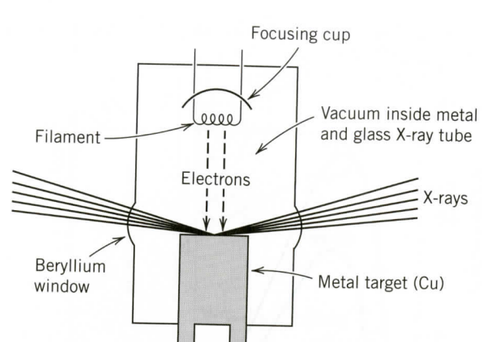

FIG. 14.2 Schematic representation of a sealed vacuum X-ray tube. The tungsten filament is heated to very high temperature, making electrons boil off. The differential voltage between the filament and the target metal accelerates the electrons toward the target. When the electrons strike the target, X-rays are produced that leave the X-ray tube housing through beryllium windows.

radiation whose wavelengths are of the order of 10^{-12} meters (see Figs. 10.24 and 14.1). All forms of electromagnetic radiation have certain properties in common, such as propagation along straight lines at a speed of 300,000 km per second in a vacuum, reflection, refraction according to Snell's law (in Chapter 13), diffraction at edges and by slits or gratings, and a relation between energy and wavelength given by the Einstein equation:

$$E = h\nu = hc/\lambda$$

where E is energy, ν is frequency, c is velocity of propagation, λ is wavelength, and h is Planck's constant. This equation shows that the shorter the wavelength the greater its energy, thus, the greater its powers of penetration. X-rays occupy only a small portion of the electromagnetic spectrum, with wavelengths ranging between slightly more than 100 Å and 0.02 Å (Fig. 14.1). X-rays used in the investigation of crystals have wavelengths on the order of 1 Å, similar in magnitude to the size of a unit cell. Visible light has wavelengths between 7,200 and 4,000 Å (720–400 nm), more than 1,000 times as great; therefore, it is less penetrative and less energetic than X-radiation.

When electrons moving at high velocity strike the atoms of any element, X-rays are produced. This is the case in an X-ray tube where electrons bombard a target material (Fig. 14.2). These X-rays result in two types of X-ray spectra: **continuous** and **characteristic** (Fig. 14.3).

A high vacuum exists in an X-ray tube. The tube is fitted with a tungsten filament as a cathode that provides the source of electrons. The anode consists of a single metal, such as Mo, Cu, or Fe, and acts as the target for the electrons. When the filament is heated by passage of a current, electrons are emitted that are accelerated toward the target anode by a high voltage applied across the tube. X-rays are generated when the source electrons impact the target (anode). The wavelength of the X-rays depends on the metal of the target and on the applied voltage. No X-rays are produced until the voltage reaches a minimum value dependent on the target material. At that voltage, a **continuous spectrum** is generated. With increasing accelerating potential, the intensity of all wavelengths increases, and the minimum wavelength of the continuous spectrum decreases (Fig. 14.3a). The *continuous spectrum*, also referred to as *white radiation*, is caused by the stepwise loss of energy of bombarding electrons in series of encounters with atoms of the target material. When an electron is instantaneously stopped, it loses all its energy at once, and the X-radiation emitted is that of the shortest wavelength (Fig. 14.3a). The stepwise energy losses from a stream of electrons produce a continuous range of wavelengths that can be plotted as a continuous function of intensity against wavelength (Fig. 14.3a). The curves begin at the short wavelength limit, rise to a maximum, and extend toward infinity at very low intensity levels.

If the voltage across the X-ray tube is increased to a critical level, which is dependent on the element of the

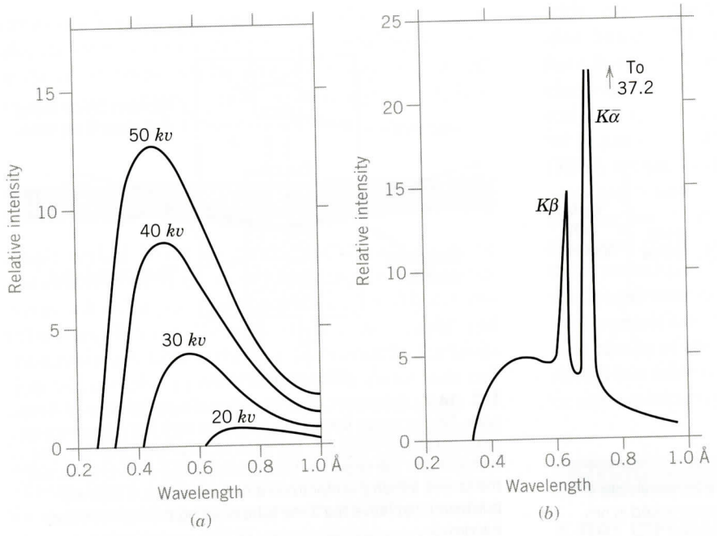

FIG. 14.3 X-ray spectra. (a) Distribution of intensity with wavelength in the continuous X-ray spectrum of tungsten at various voltages. (b) Intensity curve showing characteristic wavelengths superimposed on the continuous X-ray spectrum of molybdenum. (After Ulrey, C. T. 1918. An experimental investigation of the energy in the continuous X-ray spectra of certain elements. *Physics Reviews* 11: 401–10.)

target, a *line spectrum* of **characteristic radiation** specific to the target material becomes superimposed on the continuous spectrum. This characteristic radiation, many times more intense than the continuous spectrum, consists of several isolated, discrete wavelengths, as shown in Fig. 14.3b by *K*β and *K*α peaks.

The characteristic X-ray spectrum is produced when the bombarding electrons have sufficient energy to dislodge inner shell electrons in atoms of the target material. When these inner electrons are expelled, they leave vacancies that are filled by electrons from surrounding electron shells. The electron transitions, from outer to inner shells, are accompanied by the emission of X-radiation with specific energy (wavelength). Electrons falling from the *L*- to the *K*-shell produce $K\overline{\alpha}$ radiation, and those from the *M*- to the *K*-shell cause *K*β radiation (Fig. 14.4). The *K*β peak can be eliminated by an appropriate filter to yield essentially a single X-ray wavelength. By analogy to monochromatic light, this is called **monochromatic X-radiation**. The $K\overline{\alpha}$ radiation consists of the weighted average of two peaks, $K\alpha_1$ and $K\alpha_2$, which are very close together in wavelength.

The wavelengths of the characteristic X-radiation emitted by various metals have been accurately determined. The $K\overline{\alpha}$ wavelengths of the most commonly used anode metals are:

	Å		Å
Molybdenum	0.7107	Cobalt	1.7902
Copper	1.5418	Iron	1.9373
		Chromium	2.2909

FIG. 14.4 Schematic illustration of the production of *K* and *L* characteristic spectra as a result of electrons cascading from upper to lower energy levels in the atomic structure. X-ray emission lines are labeled with a capital letter representing the shell whose vacancy is being filled. The Greek letter is α if the electron that fills the vacancy originates in the next highest shell, β if the electron comes from two shells up, and so on. The Arabic numeral subscripts indicate specific subshells (1 for *s*, 2 for *p*) for the origin of the electron that fills the vacancy.

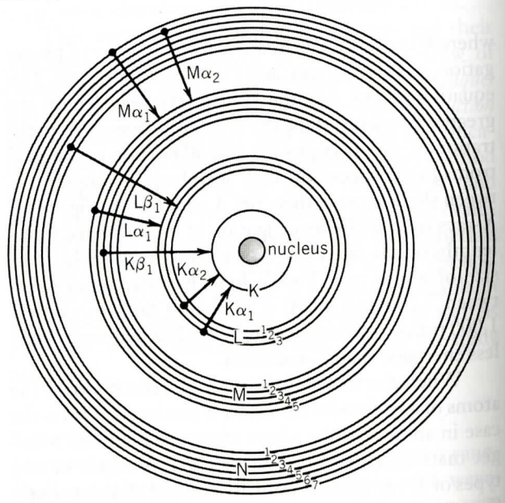

Diffraction Effects and the Bragg Equation

Minerals consist of an ordered three-dimensional structure with characteristic periodicities along the crystallographic axes. When an X-ray beam strikes such a three-dimensional orderly arrangement, it causes electrons in its path to vibrate with a frequency of the incident X-radiation. These vibrating electrons absorb some of the X-ray energy and, acting as a source for new wave fronts, emit (scatter) this energy as X-radiation of the same frequency and wavelength. In general, the scattered waves interfere destructively, but in some specific directions, they reinforce one another (interfere constructively), to produce a cooperative scattering effect known as **diffraction**.

In a row of regularly spaced atoms that is bombarded by X-rays, every atom can be considered the center of radiating, spherical wave shells (Fig. 14.5). When the scattered waves interfere constructively, they produce wave fronts that are *in phase*, and diffraction will occur. Figure 14.6 illustrates that rays 1 and 2 will be in phase only when distance *AB* represents an integral number of wavelengths; in other words, when $AB = n\lambda = c\cos\phi$ (where *n* represents whole numbers, such as 0, 1, 2, 3, . . . , *n*). For a specific value of $n\lambda$, ϕ is constant, and the locus of all possible diffracted rays will be represented by a cone with the row of scattering points as the central axis. Because the scattered rays will be in phase for the same angle ϕ on the other side of the incident beam, there will be another similar but

FIG. 14.5 Scattering of X-rays by a row of equally spaced, identical atoms.

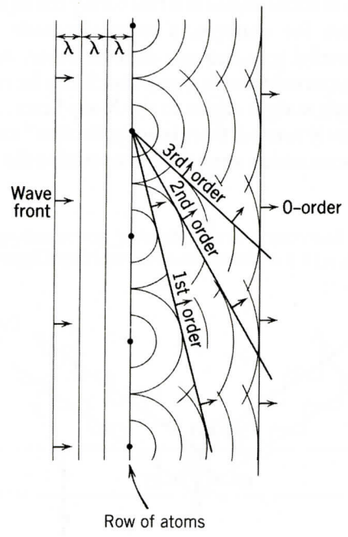

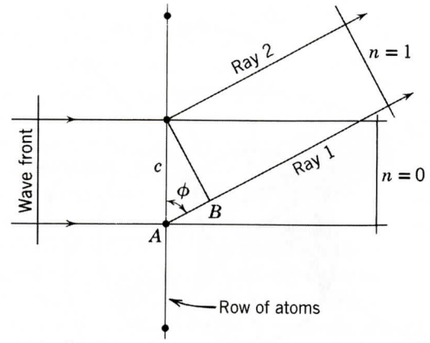

FIG. 14.6 Conditions for X-ray diffraction from a row of atoms.

inverted cone on that side (Fig. 14.7). The two cones with $n = 1$ would have ϕ (as in Fig. 14.7) as the angle between the cone axis and the outer surface of the cone. When $n = 0$, the cone becomes a plane that includes the incident beam. The greater the value of *n*, the larger is the value of cos ϕ; the smaller the angle ϕ, the narrower the cone. All have the same axis, however, and all have their vertices at the same point, the intersection of the incident beam and the row of atoms.

In a three-dimensional lattice there are three axial directions, each with its characteristic periodicity of scattering points and each capable of generating its own series of nested cones with characteristic apical angles. Diffraction cones from any three noncoplanar rows of scattering atoms may or may not intersect each other, but only when all three intersect in a common line is there a diffracted beam (Fig. 14.8). This direction (shown by the arrow in Fig. 14.8) represents the

FIG. 14.7 Diffraction cones from a row of atoms.

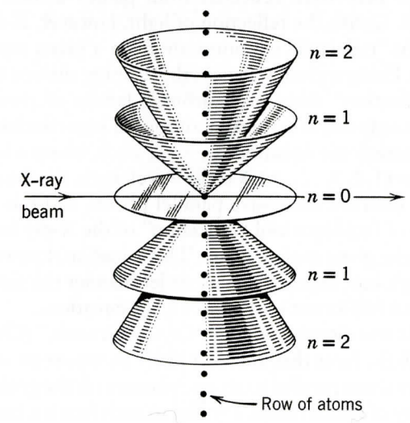

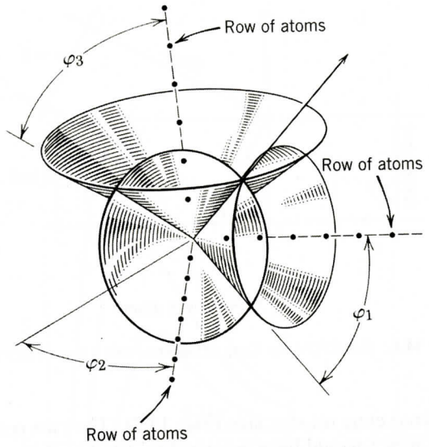

FIG. 14.8 Diffraction cones from three noncoplanar rows of scattering atoms, intersecting in a common line.

direction of the diffracted beam, which can be recorded on a film or registered electronically. The geometry of the three intersecting cones in Fig. 14.8 can be expressed by three independent equations (the Laue equations) in which the three cone angles (ϕ_1, ϕ_2, and ϕ_3) define a common direction along the path of the arrow (the common intersection of the three cones). In order to produce a diffraction effect (a spot on a photographic plate or film), these three geometric equations must be simultaneously satisfied. The three equations are named after Max von Laue, who originally formulated them.

Shortly after the publication of these equations, W. L. Bragg pointed out that although X-rays are indeed diffracted by crystals, the diffracted X-rays act as though they were reflected from planes within the crystal. Unlike the reflection of light, however, X-rays are not "reflected" continuously from a given crystal plane. Using a given wavelength, λ, Bragg showed that a "reflection" takes place from a family of parallel planes only under certain conditions. These conditions must satisfy the equation: $n\lambda = 2d \sin \theta$, where n is an integer (1, 2, 3, . . . , n), λ is the wavelength, d is the distance between successive parallel planes, and θ is the angle of incidence and "reflection" of the X-ray beam from the given atomic plane. This equation, known as **Bragg's law**, expresses in a simpler manner the simultaneous fulfillment of the three Laue equations.

As was discussed under "Crystal Growth," (Chapter 10) the faces that are most likely to appear on crystals are those parallel to atomic planes with the greatest density of lattice nodes. Parallel to each face is a family of equally spaced identical planes. When an X-ray beam strikes a crystal, it penetrates it, and the resulting diffraction effect is not from a single plane but from an almost infinite number of parallel planes (inside the structure), each contributing a small bit to the total diffraction maximum. In order for the diffraction effect ("reflection") to be of sufficient intensity to be recorded, the individual "reflections" must be *in phase* with one another. The following conditions necessary for reinforcement were demonstrated by W. L. Bragg.

In Fig. 14.9, the lines p, p_1, and p_2 represent the traces of a family of atomic planes with spacing d. X-rays striking the outer plane pp would be reflected at the incident angle θ, whatever the value of θ. However, to reinforce one another in order to give a "reflection" that can be recorded, all "reflected" rays must be *in phase*. The path of the waves along DEF "reflected" at E is longer than the path of the waves along ABC "reflected" at B. If the two sets of waves are to be *in phase*, the path difference of ABC and DEF must be a whole number of wavelengths ($n\lambda$). In Fig. 14.9, BG and BH are drawn perpendicular to AB and BC, respectively, so that $AB = DG$ and $BC = HF$. To satisfy the condition that the two waves be in phase, $GE + EH$ must be equal to an integral number of wavelengths. BE is perpendicular to the lines p and p_1 and is equal to the interplanar spacing d. In ΔGBE, $d \sin \theta = GE$; and, in ΔHBE, $d \sin \theta = EH$. Thus, for in phase "reflection," $GE + EH = 2d \sin \theta = n\lambda$. This equation,

$$n\lambda = 2d \sin \theta$$

is the **Bragg equation**. For a given interplanar spacing (d) and a given λ, "reflections" (diffraction maxima) occur only at those angles of θ that satisfy the equation.

Suppose for example, a monochromatic X-ray beam is parallel to a cleavage plate of halite, and the plate is supported in such a way that it can be rotated about an axis at right angles to the X-ray beam. As the halite is slowly rotated, there is no "reflection" until the incident beam makes an angle θ that satisfies the Bragg

FIG. 14.9 Geometry of X-ray "reflection" from equally spaced planes (p, p_1, p_2) in a crystal structure with spacing d between them.

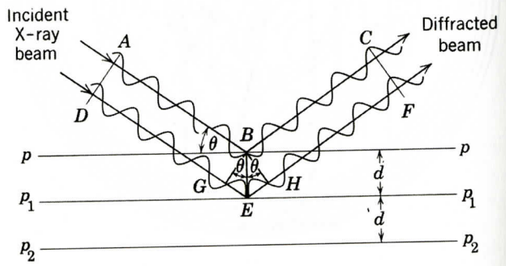

equation, with $n = 1$. On continued rotation, there are additional "reflections" only when the equation is satisfied at certain θ angles with $n = 2, 3, \ldots$. These are known as the first-, second-, third-order, etc., "reflections." These "reflections" are the diffraction effects that occur when the three diffraction cones about three noncoplanar rows of atoms intersect in a common direction (Fig. 14.8). This diffraction process is the basis for single crystal and powder X-ray techniques.

Single-Crystal X-ray Diffraction and Structure Analysis

Single-crystal X-ray diffraction, as the name implies, is the interaction of an X-ray beam with a very small single-crystal (about 1 mm in size or smaller) of a mineral (or other crystalline substance). The interaction of the X-ray beam and the crystalline structure produces X-ray diffraction effects that can be recorded on film or measured by an electronic device, such as an X-ray counter (or detector). Until 1970, almost all X-ray diffraction studies involved film methods that consisted of a crystal positioned in an X-ray beam at a fixed distance from a film wrapped in a light-tight envelope. Figure 14.10a shows this arrangement for the *Laue method* in which the crystal is stationary and the X-ray beam is unfiltered (meaning that it contains X-rays represented by $K\beta$ radiation as well as the continuum in addition to the $K\alpha$ radiation). Although the Laue method is now mainly of historic interest, it is mentioned here because the resulting diffraction effects, as recorded on a flat film, display the symmetry of the crystal as long as one of the crystallographic axes of the crystal is aligned parallel with the X-ray beam. Figure 14.10b illustrates the four-fold symmetry arrangement of X-ray diffraction spots (about the center of the film) for the tetragonal mineral vesuvianite. Here, the X-ray beam was parallel to the c axis, the four-fold axis in vesuvianite.

In other single-crystal film methods, the film is generally not stationary, and furthermore, the film may not be contained in a flat but instead in a cylindrical housing. The most commonly used single-crystal method in which a flat film and a single crystal move in a complex gyratory motion, is known as the *precession method*. An example of an X-ray single-crystal precession photograph of vesuvianite is shown in Fig. 14.11.

Although enormous numbers of crystal structures have been solved on the basis of data obtained on film using single-crystal camera techniques, the modern approach to data acquisition is by a *single-crystal diffractometer*. In such instrumentation (see also "X-ray

FIG. 14.10 (a) Obtaining a Laue photograph with a stationary crystal. (b) Laue photograph of vesuvianite with point group symmetry 4/*m*2/*m*2/*m*. The photograph was taken along the four-fold rotation axis (*c* axis) of vesuvianite, thus, revealing four-fold symmetry and mirrors in the arrangement of diffraction spots. The axial directions, a_1 and a_2, were inked onto the photograph after it had been developed.

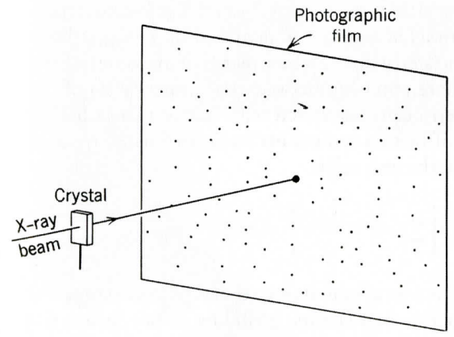

(a)

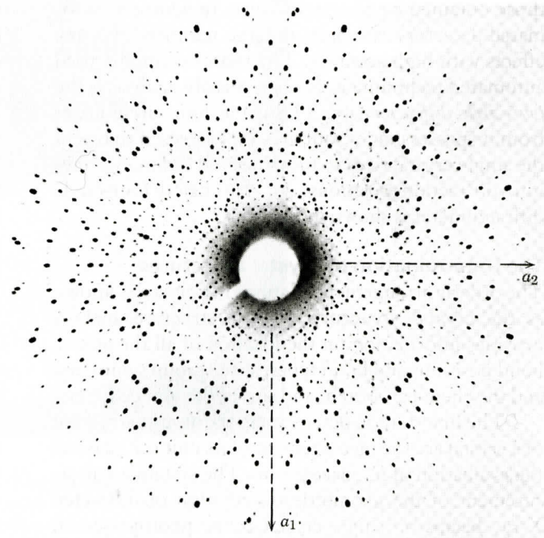

(b)

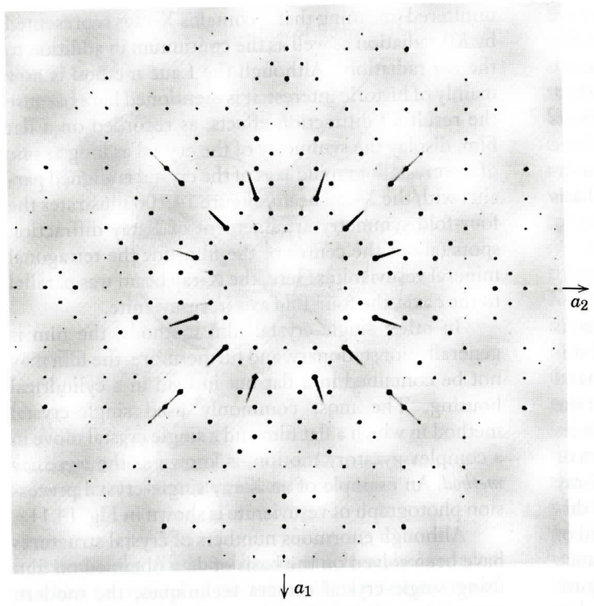

FIG. 14.11 Precession photograph of vesuvianite, with point group symmetry 4/*m*2/*m*2/*m*. The photo was taken along the four-fold rotation *c* axis, thus, revealing the four-fold symmetry about the axis, as well as the mirror planes. Compare with Fig. 14.10b.

Powder Diffraction and Mineral Identification" later in this chapter), the intensity of X-ray diffraction maxima is not evaluated from the intensity of a spot on an X-ray film, but instead is measured by an X-ray counter (or detector). Such detectors greatly improve the accuracy of X-ray intensity measurements over those obtained by film techniques. In addition, automated detectors can measure large numbers of X-ray effects with high accuracy. The most commonly used automated technique in X-ray structure analysis is the *four-circle diffractometer*. The name four-circle arises from its possession of four arcs that are used to orient the single crystal so as to bring desired (atomic) planes into diffraction positions. An automated four-circle diffractometer is shown in Fig. 14.12.

The Determination of Crystal Structures

The orderly arrangement of atoms in a crystal is known as the **crystal structure**. Crystal structure analysis provides information on the location of all the atoms, bond positions and bond types, space group symmetry, and the chemical content and size of the unit cell.

The first steps in determining the atomic structure of a crystal are the measurement of its unit cell size and the evaluation of its space group. The systematic measurement of the geometric distribution of diffracted X-ray beams on single crystal X-ray photographs in one or more crystallographic orientations (precession photographs are most convenient) yields information about the geometry of that crystal's unit cell, specifically the lengths of the unit cell edges and the angles between them. Information about the space group and the crystal structure (i.e., the symmetry of the atomic arrangement and the coordinates of atoms within the unit cell) is contained in the intensities of the diffracted beams, which are measured either from X-ray single crystal photographs, or more commonly with quantum counting detectors on single-crystal diffractometers. The diffracted beams are identified by Bragg indices, *hkl*, associated with the lattice planes of the same indices.

The relationship between the intensity (I) of the diffracted beam associated with lattice planes having Bragg diffraction indices *hkl* and coordinates $x_j y_j z_j$ of atom j in the unit cell is

$$I = k\left[\sum_j f_j e^{i2\pi(hx_j+ky_j+lz_j)}\right]^2 = kF_{hkl}^2$$

where k is a term containing several physical constants and experimental factors, including a scale factor; f_j is the scattering factor of atom j (which depends on atomic number and scattering angle and includes corrections for atomic thermal motion); and the summation is over all atoms in the unit cell. The summation is termed the **structure factor**, F_{hkl}, and its value depends on the kinds of atoms in the unit cell and their positions.

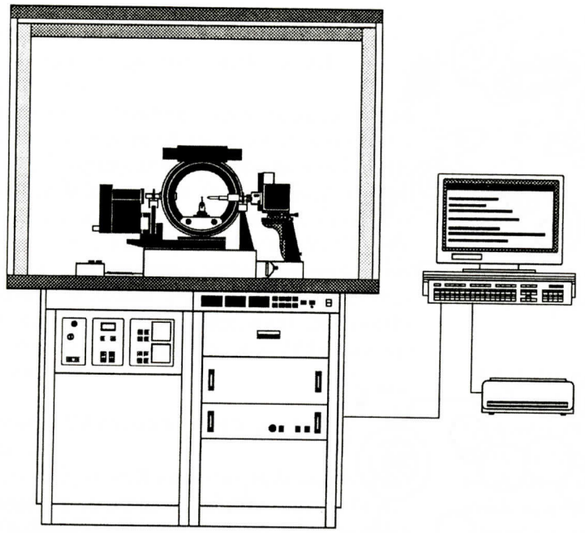

(*a*)

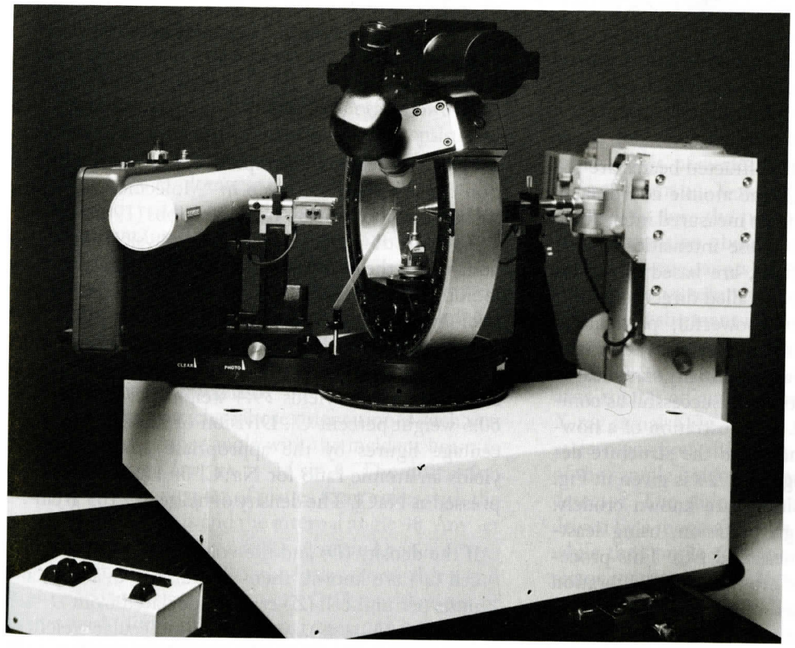

(*b*)

FIG. 14.12 (a) Schematic illustration of the P4 single-crystal X-ray diffractometer manufactured by Siemens Industrial Automation. (b) Close-up of the four-circle goniometer for controlling the orientation of the single crystal (in the center of the photograph). To the right is the X-ray tube, and to the left is the X-ray detector, a scintillation counter. (Courtesy of Siemens Industrial Automation, Inc., Madison, Wisconsin.)

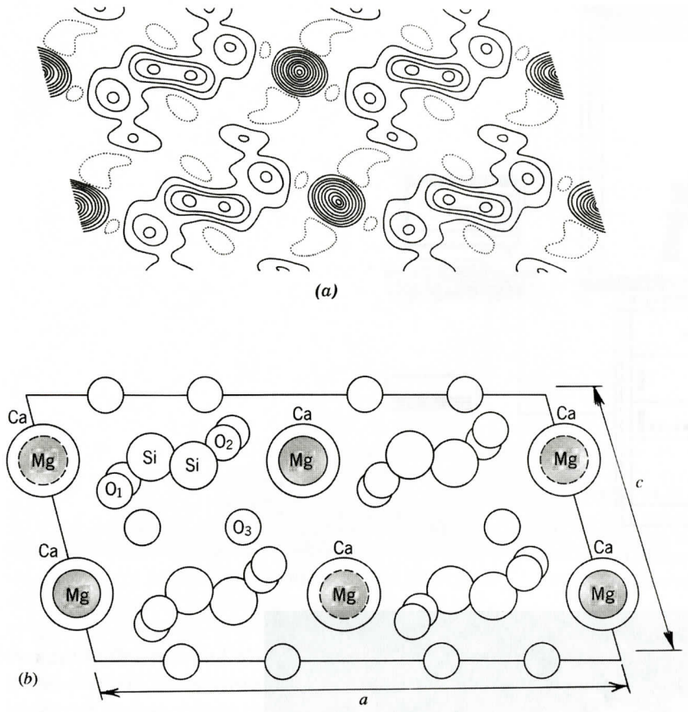

FIG. 14.13 (a) The summation of Fourier series for diopside, $CaMgSi_2O_6$, projected on (010). The distribution of scattering matter is indicated by contour lines drawn through points of equal density in the projection. (b) The atomic positions of diopside (with space group *C* 2/*c*) projected on (010), as derived from the distribution in (a). (Redrawn after Bragg, W. L. 1929. *Zeitschrift für Kristallographie* 70:488.)

Because the intensities of diffracted beams are related to F^2_{bkl} rather than F_{bkl}, the atomic coordinates cannot be extracted directly from measured intensities. Current methods, by which these intensities can be made to yield atomic positions, are based either on using Fourier techniques or so-called direct methods. Fourier techniques are very powerful, particularly when the positions of a small number of heavy atoms are known. Direct methods are essentially statistical in nature and have become extremely successful as computing power has increased. An illustration of a now-classical electron density map (and the structure derived from it) by W. L. Bragg in 1929 is given in Fig. 14.13. Once the atom positions are known crudely, they can be refined to high precision, using least-squares analysis on many measured F^2_{bkl}. This procedure can yield amplitudes of atomic thermal vibration as well as site occupancies of substituting atomic species in minerals that are members of a solid solution series. Accurate interatomic distances (bond lengths) can then be calculated from refined atomic coordinates. In recent years, highly accurate electron density maps, calculated as a Fourier series in which the structure factors are the Fourier coefficients, have yielded information about bonding and the spatial distribution of valence electrons. Examples of such detailed electron density maps are given in "Molecules as models for bonding in silicates," by G. V. Gibbs (1982).

To illustrate the chemical and physical interrelationships in the derivation of a simple crystal structure, sodium chloride (NaCl) is used. The external morphology of halite is consistent with isometric symmetry (point group: $4/m\bar{3}2/m$). X-ray diffraction data indicate that the unit cell has an edge dimension (a) of 5.64 Å. A chemical analysis yields 39.4 weight percent Na and 60.6 weight percent Cl. Division of these weight percentage figures by the appropriate atomic weights yields an atomic ratio for Na:Cl or 1:1, which is expressed as NaCl. The density of halite is 2.165 g/cm^3.

If the density (D) and the volume (V) of the unit cell (a^3) are known, then the number of formula units per unit cell (Z) can be calculated from $D = (Z \times M)/(N \times V)$, where M is molecular weight and N is Avogadro's number (6.02338×10^{23}).

The number of formula units per unit cell for halite is four, which means that the unit cell contains four NaCl units, or four Na^+ and four Cl^- ions. It is now possible to assess the structural arrangement of the ions in NaCl. The radius ratio of Na^+ to Cl^- would predict a coordination of six about each of the ions. A reasonable, and correct, interpretation of the crystal structure is given in Fig. 4.17.

Supplementing structure analyses based on diffraction phenomena (these are X-ray, neutron, and electron diffraction techniques), a variety of spectroscopic methods (that provide information about the local environments or ionization states of certain atomic species) are used. Spectroscopic techniques include infrared, optical, Mössbauer, and resonance techniques, such as nuclear magnetic resonance (NMR). Thus, a complete structural picture of a mineral at the atomic level usually requires information obtained by both diffraction and spectroscopy.

X-ray Powder Diffraction and Mineral Identification

The relative rarity of well-formed crystals and the difficulty of achieving the precise orientation required by single-crystal methods led to the discovery of the **powder method** of X-ray investigation. In X-ray diffraction studies of powders, the original specimen is prepared by grinding it to a fine powder, which is bonded with an amorphous material into a small spindle (for powder film methods) or spread uniformly over the surface of a glass slide. If sufficient powder is available, it can be packed into a special rectangular sample holder (for powder diffractometer techniques). The *powder mount* consists ideally of crystalline particles in completely random orientation. To ensure randomness of orientation of these tiny particles with respect to the impinging X-ray beam, the spindle mount (used in film cameras) is generally rotated in the path of the beam during exposure.

When a beam of monochromatic X-rays strikes the mount, all possible diffractions take place simultaneously. If the orientation of the crystalline particles in the mount is truly random, for each family of atomic planes with its characteristic interplanar spacing (d), there are many particles whose orientation is such that they make the proper angle with the incident beam to satisfy the *Bragg law*: $n\lambda = 2d \sin \theta$. The diffraction maxima from a given set of planes form cones with the incident beam as axis and the internal angle 4θ. Any set of atomic planes yields a series of nested cones corresponding to "reflections" of the first, second, third, and higher orders ($n = 1, 2, 3, \ldots$). Different families of planes with different interplanar spacings will satisfy the Bragg law at appropriate values of θ for different integral values of n, thus, giving rise to separate sets of nested cones of "reflected" rays.

If the rays forming these cones are permitted to fall on a flat photographic plate at right angles to the incident beam, a series of concentric circles will result (Fig. 14.14). However, only "reflections" with small values of the angle 2θ can be recorded in this manner. In order to record all the possible diffraction cones that may occur in three dimensions (Figs. 14.7 and 14.8), a film method is used in which the film is wrapped around the inside of a cylindrical camera. This camera is known as a *powder camera* in which the film fits snugly to the inner curve of the camera (Fig. 14.15a). This type of mounting is known as the *Straumanis method*. Figure 14.15b shows the circular film strip with two holes cut into it, one to allow the X-ray beam to enter the camera and the other for a lead-lined beam catcher. Although this powder camera method has been used extensively for mineral identification, the X-ray *powder diffractometer* is the instrumental method currently used most often. This powerful analytical tool uses essentially monochromatic X-radiation and a finely powdered sample, as does the powder film method, but records the information about the "reflections" as electronic counts (X-ray counts) that are stored and graphically displayed on a computer screen.

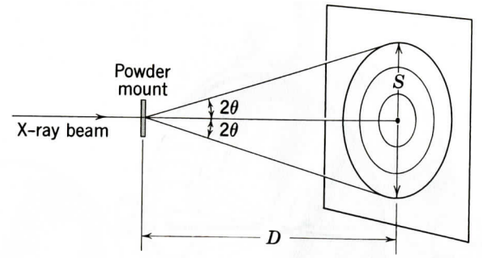

FIG. 14.14 X-ray diffraction from a powder mount recorded on a flat photographic plate inside a light-tight envelope.

The instrument is constructed such that when the sample is in place, it rotates in the path of a collimated X-ray beam while an X-ray detector, mounted on an arm, rotates about the sample to collect the diffracted X-ray signals (Fig. 14.16). When the instrument is set at zero position, the X-ray beam is parallel to the base of the sample holder and passes directly into the X-ray detector. The slide mount and the X-ray counter are driven by a motor through separate gear trains so that, while the sample rotates through the angle θ, the detector rotates through 2θ.

If the specimen has been properly prepared, there will be thousands of tiny crystalline particles in random orientation. As in powder photography, all possible "reflections" from atomic planes take place simultaneously. Instead of recording all of them on a film at one time, however, the X-ray detector maintains the appropriate geometrical relationship to receive each diffraction maximum separately.

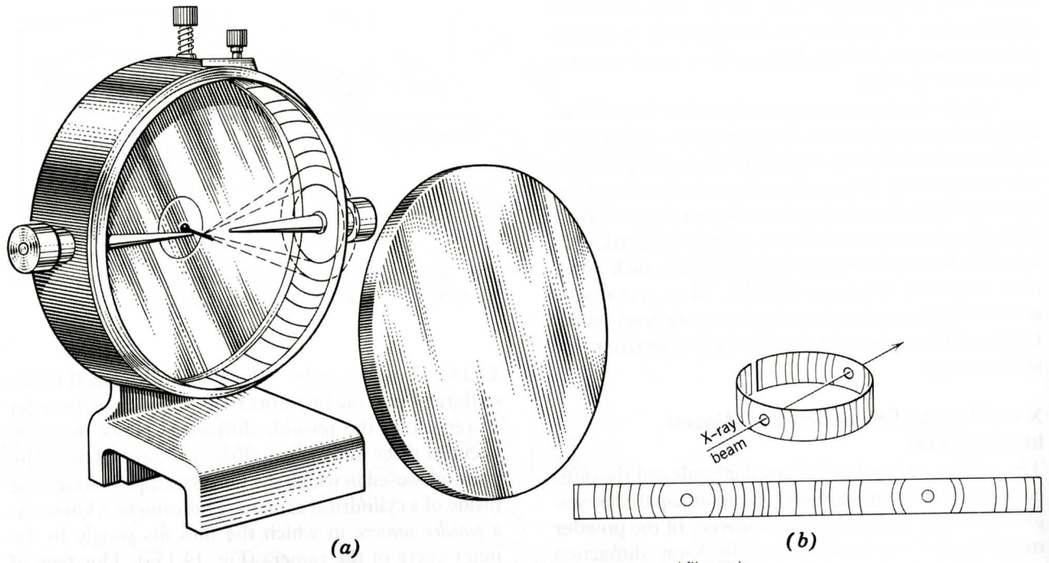

FIG. 14.15 (a) Metal powder diffraction camera with a powder spindle in the center and film strip against the inner cylindrical wall of the camera. (b) Circular film strip with curved lines that represent the conical "reflections" produced inside the camera.

In operation, the sample, the X-ray detector, and the recording device are activated simultaneously. If an atomic plane has an interplanar spacing (d) such that a reflection occurs at $\theta = 20°$, there is no evidence of this reflection until the counting tube has been rotated through 2θ, or 40°. At this point, the diffracted beam enters the X-ray detector, causing it to respond. The pulse generated is amplified and causes an electronic response on a vertical scale that represents peak height. The angle 2θ at which the diffraction occurs is read on a horizontal scale. The heights of the peaks are directly proportional to the intensities of the diffraction effects.

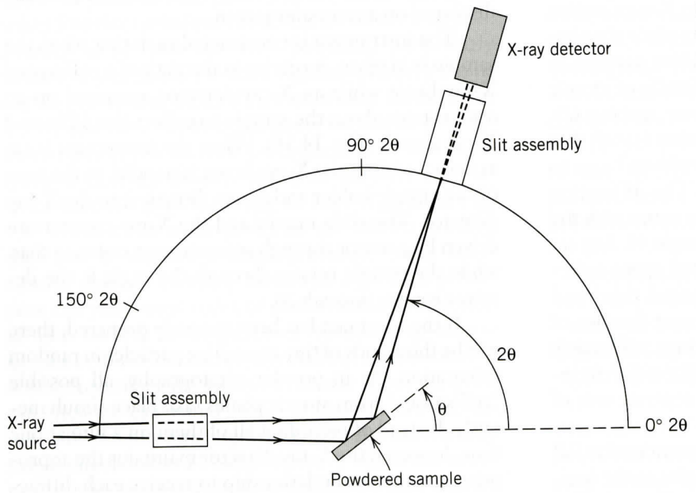

FIG. 14.16 Schematic illustration of the essential components of a powder X-ray diffractometer. In such an instrument the sample holder rotates at $\theta°$ while the detector arm rotates $2\theta°$.

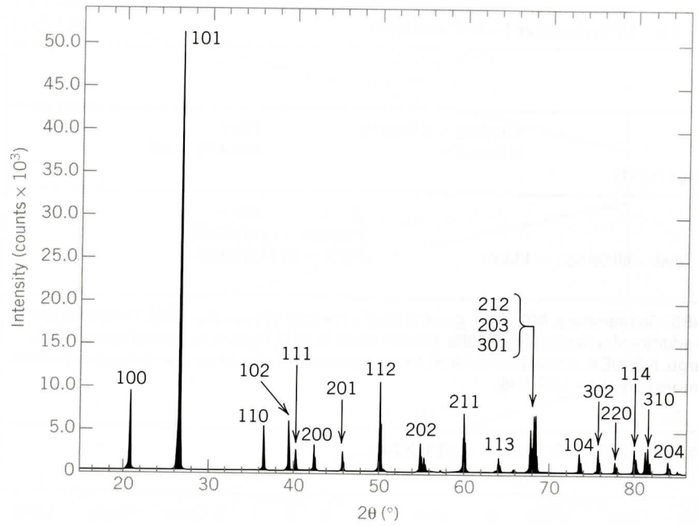

FIG. 14.17 X-ray powder diffractometer tracing for a finely powdered sample of low quartz. Peaks are indexed with the appropriate *hkl* responsible for the "reflection."

An example of a diffractometer tracing for low quartz is given in Fig. 14.17. The 2θ positions of the diffraction peaks in such a tracing can be read off directly or they can be tabulated as 2θ positions by an online computer. The interplanar spacings giving rise to them are calculated using the equation $n\lambda = 2d \sin \theta$.

Once a diffractometer tracing has been obtained and the various diffraction peaks have been tabulated in a sequence of decreasing interplanar spacings (d), together with their relative intensities (I, with the strongest peak represented by 100 and all the other peaks scaled with respect to 100), the investigator can begin the mineral identification process. Through a computer search technique (searching for comparable or identical diffraction patterns on the basis of the strongest lines or the largest interplanar spacings), the diffraction pattern of an unknown can be compared with records stored in the Powder Diffraction File (PDF) published by the International Center for Diffraction Data (ICDD). (This database is available in electronic format from the ICDD.)

The PDF is the world's largest and most complete collection of X-ray powder diffraction patterns, containing more than 217,000 calculated and experimental patterns for natural and synthetic crystalline materials compiled by the ICDD since 1941. Each pattern includes a table of interplanar (d) spacings, relative intensities (I), and Miller indices, as well as additional information, such as chemical formula, compound name, mineral name, structural formula, crystal system, physical data, experimental parameters, and references. An example printout for low quartz from this file is shown in Fig. 14.18. Entries are indexed to allow for topical searches of inorganics, organics, minerals, metals and alloys, pharmaceuticals, zeolites, and many others. By this automated search procedure, a completely unknown substance can be identified in a short time using a very small volume of sample.

The powder method is of wider usefulness, however, and there are several other valuable applications. Variations in chemical composition of a known substance involve the substitution of ions, generally of a somewhat different size, in specific sites in a crystal structure. As a result of this substitution, the unit cell dimensions, and, consequently, the interplanar spacings, are slightly changed. Commensurate with the changes in interplanar spacing, the positions of the lines in the powder diffractogram shift accordingly. By measuring these small shifts in position of the lines in powder patterns of substances of known structure, changes in chemical composition may be accurately detected. Figure 14.19 illustrates a variation diagram that correlates unit cell dimensions (b and unit cell volume, V) and changes in the position of a specific diffraction maximum (1,11,0) with composition for members of the cummingtonite-grunerite (amphibole) series.

Further, the relative proportions of two or more known minerals in a mixture may be determined by the comparison of the intensities of the same peaks in diffractometer patterns of prepared control samples of

PDF#33-=1161 (Deleted Card): QM = Star (+); d = Diffractometer, I = Diffractometer — PDF Card

Quartz, syn
SiO2

Radiation = CuKa1 — Lambda = 1.540598 — Filter =
Calibration = Internal (Si) — d-Cutoff = — I/Ic (RIR) = 3.6
Ref = Natl. Bur. Stand. (U.S.) Mongr. 25, 18 61 (1981)

Hexagonal—(Unknown), P3221(154) — Z = 3 — mp =
Cell = 4.9134 × 5.4053 — Pearson = hP9 (O2 Si)
Censity (c) = 2.649 Density (m) = 2.656 Mwt = 60.08 Vol. = 113.01 — F(30) = 76.8 (.0126,31)
Ref = Ibid.

NOTE: Sample from the Glass Section at NBS, Gaithersburg, MD, USA, ground single-crystals of optical quality. To replace 5-490 and validated by calculated pattern. Plus 6 additional reflections to 0.9089. Pattern taken at 25 C. Pattern reviewed by Hozler, J., McCarthy, G., North Dakota State Univ., Fargo, ND, USA, ICDD Grant-in-Aid (1990). Agrees well with experimental and calculated patterns. Deleted by 46-1045, higher F#N, more complete, LRB 1/95.
Color: Colorless

Strong Line: 3.34/X 4.26/2 1.82/1 1.54/1 2.46/1 2.28/1 1.37/1 1.38/1 2.13/1 2.24/1
39 Lines, Wavelength to Compute Theta = 1.54056A (Cu), 1%-Type = (Unknown)

#	d(A)	I(f)	h	k	l	2-Theta	Theta	1/(2d)	#	d(A)	I(f)	h	k	l	2-Theta	Theta	1/(2d)
1	4.2570	22.0	1	0	0	20.850	10.425	0.1175	21	1.2285	1.0	2	2	0	77.660	38.830	0.4070
2	3.3420	100.0	1	0	1	26.651	13.326	0.1495	22	1.1999	2.0	2	1	3	79.875	39.938	0.4167
3	2.4570	8.0	1	1	0	36.541	18.271	0.2035	23	1.1978	1.0	2	2	1	80.044	40.022	0.4174
4	2.2820	8.0	1	0	2	39.455	19.727	0.2191	24	1.1843	3.0	1	1	4	81.145	40.572	0.4222
5	2.2370	4.0	1	1	1	40.283	20.141	0.2235	25	1.1804	3.0	3	1	0	81.470	40.735	0.4236
6	2.1270	6.0	2	0	0	42.464	21.232	0.2351	26	1.1532	1.0	3	1	1	83.818	41.909	0.4336
7	1.9792	4.0	2	0	1	45.808	22.904	0.2526	27	1.1405	1.0	2	0	4	84.969	42.484	0.4384
8	1.8179	14.0	1	1	2	50.139	25.070	0.2750	28	1.1143	1.0	3	0	3	87.451	43.731	0.4487
9	1.8021	1.0	0	0	3	50.610	25.305	0.2775	29	1.0813	2.0	3	1	2	90.855	45.428	0.4624
10	1.6719	4.0	2	0	2	54.867	27.434	0.2991	30	1.0635	1.0	4	0	0	92.819	46.410	0.4701
11	1.6591	2.0	1	0	3	55.327	27.663	0.3014	31	1.0476	1.0	1	0	5	94.662	47.331	0.4773
12	1.6082	1.0	2	1	0	57.236	28.618	0.3109	32	1.0438	1.0	4	0	1	95.115	47.558	0.4790
13	1.5418	9.0	2	1	1	59.947	29.973	0.3243	33	1.0347	1.0	2	1	4	96.223	48.112	0.4832
14	1.4536	1.0	1	1	3	63.999	32.000	0.3440	34	1.0150	1.0	2	2	3	98.734	49.367	0.4926
15	1.4189	1.0	3	0	0	65.759	32.879	0.3524	35	0.9898	1.0	4	0	2	102.195	51.098	0.5052
16	1.3820	6.0	2	1	2	67.748	33.874	0.3618	36	0.9873	1.0	3	1	3	102.556	51.278	0.5064
17	1.3752	7.0	2	0	3	68.128	34.064	0.3636	37	0.9783	1.0	3	0	4	103.880	51.940	0.5111
18	1.3718	8.0	3	0	1	68.321	34.160	0.3645	38	0.9762	1.0	3	2	0	104.195	52.098	0.5122
19	1.2880	2.0	1	0	4	73.460	36.730	0.3882	39	0.9636	1.0	2	0	5	106.141	53.071	0.5189
20	1.2558	2.0	3	0	2	75.668	37.834	0.3982									

FIG. 14.18 Example of the printout for SiO_2, low quartz, as obtained from the powder diffraction file (PDF-2) licensed by the International Center for Diffraction Data (JCPDS), 12 Campus Boulevard, Newton Square, PA., 19073-3273; copyright © JCDPS-ICDD, 1999. The printout was obtained using Jade 5.0 from Materials Data Inc. (MDI).

known composition. This is commonly applied to the study of fine-grained materials, such as clay minerals. For X-ray diffraction patterns of clay minerals, oriented powders are used that maximize reflection from specific and characteristic *hkl*s (mainly the 00*l* peaks). However, relating the intensity of a diffraction peak to the abundance of the material is not straightforward, and numerous factors must be taken into account (refer to Moore and Reynolds, 1997 for details).

An X-ray powder diffraction technique, the *Rietveld refinement method*, allows for the extraction of structural information from powdered instead of single-crystal specimens. This is an especially important development for the determination of crystal structures of minerals that are typically finely crystalline and are not found in well-developed single crystals. Examples of such finely crystalline or poorly ordered minerals are clay minerals, manganese and iron oxides and hydroxides,

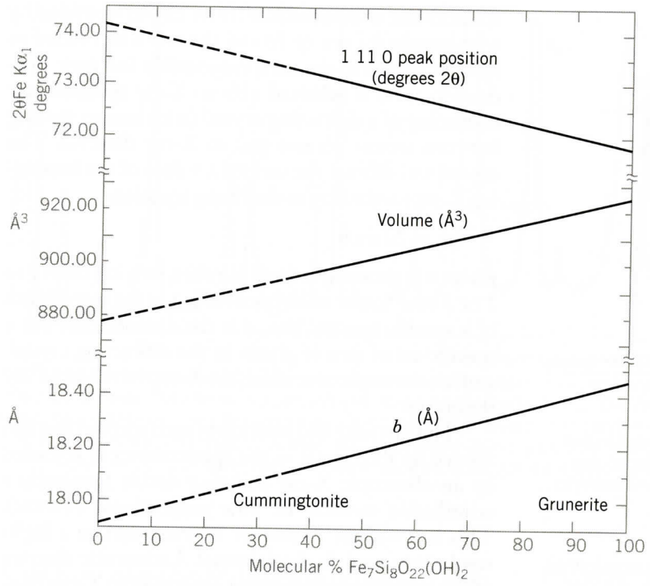

FIG. 14.19 Variation of *b* and *V* (volume) of the unit cell and the position of the 1,11,0 peak as a function of composition in the monoclinic cummingtonite–grunerite series with composition ranging from $Fe_2Mg_5Si_8O_{22}(OH)_2$ to $Fe_7Si_8O_{22}(OH)_2$. (After Klein, C., and D. R. Waldbaum. 1967. X-ray crystallographic properties of the cummingtonite-grunerite series. *Journal of Geology* 75:379–92).

and some zeolites. There are three basic requirements of the Rietveld refinement:

1. Availability of accurate powder diffraction intensity data measured at specific intervals of 2θ.
2. A basic understanding ("starting model") of the actual crystal structure of the material that is being studied.
3. A quantitative understanding of shapes, width, and any systematic errors in the positions of X-ray peaks in the powder pattern.

For further discussion of the Rietveld method, see Post and Bish (1989; see the reference list for complete reference).

Several exercises using X-ray powder diffraction film and diffractometer techniques are given in Klein (2008).

X-RAY FLUORESCENCE ANALYSIS (XRF)

This analytical technique, also known as **X-ray emission spectrography**, is used in most research laboratories that study the chemistry of inorganic substances. It is widely used by petrologists to acquire bulk chemical compositions of rocks including the abundance of rare earth elements. It is also routinely used in a wide range of industrial applications. Examples of such applications are in the mining industry (for quality control of the product shipped to the consumer), in the glass and ceramics industry, in the manufacture of metals and alloys, and in environmental-protection and pollution-control applications.

The analysis sample, in this technique, is ground to a fine powder and subsequently compressed into a circular pellet, or into a disc with the admixture of a binder. The pellet or disc of sample is irradiated (for a short period of time) with polychromatic X-rays generated in a high-intensity X-ray tube (Fig. 14.1 for the λ range of X-rays). These incident X-rays from the X-ray tube are, to a considerable extent, absorbed according to Beer's Law:

$$\log \frac{I_o}{I} = K_d \Delta d$$

where I_0 is the incident X-ray intensity, I is the intensity of the X-ray beam that was not absorbed in the sample, K_d is a proportionality constant, and Δd is the thickness of the sample. The X-ray energy that is absorbed in the sample results in the generation of an *X-ray emission spectrum that is characteristic* for each element in the sample. In the process of the absorption of X-ray energy in the sample, electrons are dislodged from the innermost shells (*K*, *L*, *M*; as discussed earlier for X-ray diffraction). An expelled electron (from, e.g., the *K*-shell) must be replaced, and it is highly probable that the vacancy will be filled from the next outer shell (the *L*-shell) rather than from a more remote shell. This creates a new vacancy, which is filled from the next shell, and so on. Electrons that "fall into" inner electron shells move